ACS Chemical Neuroscience
Cite This: ACS Chem. Neurosci. 2018, 9, 2838−2848
Research Article
pubs.acs.org/chemneuro

Peptide-Based Acetylcholinesterase Inhibitor Crosses the Blood-Brain Barrier and Promotes Neuroprotection

Prasenjit Mondal,[†,‡] Varsha Gupta,[†] Gaurav Das,[†,‡] Krishnangsu Pradhan,[†] Juhee Khan,[†] Prabir Kumar Gharai,[†] and Surajit Ghosh*[,†,‡]

[†]Organic & Medicinal Chemistry Division, CSIR-Indian Institute of Chemical Biology, 4, Raja S. C. Mullick Road, Jadavpur, Kolkata-700032, West Bengal, India

[‡]Academy of Scientific and Innovative Research (AcSIR), CSIR-Indian Institute of Chemical Biology Campus, 4 Raja S. C. Mullick Road, Kolkata 700032, India

Supporting Information

ABSTRACT: Design and development of acetylcholinesterase (AChE) inhibitor has tremendous implications in the treatment of Alzheimer's disease (AD). Here, we have adopted a computational approach for the design of a peptide based AChE inhibitor from its active site. We identified an octapeptide, which interacts with the catalytic anionic site (CAS) of AChE enzyme and inhibits its activity. Interestingly, this peptide also inhibits amyloid aggregation through its interaction at the 17−21 region of amyloid-beta (Aβ) and stabilizes microtubules by interacting with tubulin as well. Eventually, in the PC12 derived neurons, it shows noncytotoxicity, promotes neurite out-growth, stabilizes intracellular microtubules, and confers significant neuroprotection even upon withdrawal of nerve growth factor (NGF). Further, results reveal that this peptide possesses good serum stability, crosses the blood-brain barrier (BBB), and maintains the healthy architecture of the primary cortical neurons. This work shows discovery of an excellent peptide-based AChE inhibitor with additional potential as a microtubule stabilizer, which will pave the way for the development of potential anti-AD therapeutics in the near future.

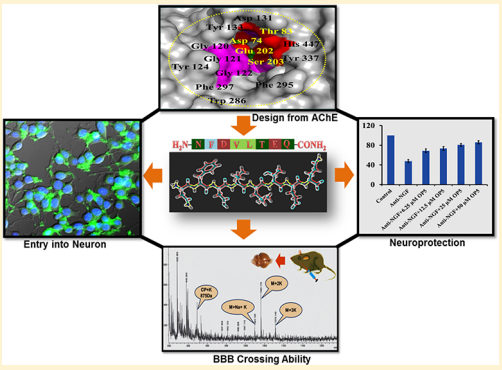

KEYWORDS: *Neuropeptide, acetylcholinesterase, amyloid-beta, Alzheimer's disease, microtubule*

1. INTRODUCTION

Alzheimer's disease (AD) is associated with progressive damage of brain cells that causes memory loss and confusion.[1] Efforts are been made to treat this devastating disease using multiple approaches that mainly focus on the development of inhibitors for β-secretase-1 (BACE-1), tau hyperphosphorylation, cholinesterase (ChE) , and Aβ aggregation.[2] However, the clinically effective therapy is rare. In this direction, only few attempts have been made for the development of inhibitors for ChE and have been considered as symptomatic treatment of AD.[3] Recently, we garnered more interest in the development of acetylcholinesterase (AChE)-targeted AD therapeutics, because of its plausible cross-talk with the amyloid-beta (Aβ) aggregation pathway.[4,5] AChE has two important binding sites, namely, the peripheral anionic site (PAS) and catalytic active site (CAS). It has been described before that CAS is positioned at the bottom and catalyzes the hydrolysis of neurotransmitter, while PAS is situated at the edge of the enzyme surface and is responsible for noncholinergic functions of AChE.[6] The detailed mechanistic insights of PAS inhibition, specifically its role in Aβ formation are poorly understood. In addition, earlier reports shows that CAS and PAS play an important role in enhancement of neurotoxicity of amyloid fibrils and coordination between AChE activity, tau hyperphosphorylation and Aβ formation, respectively.[5,7] Thus, further approaches are required to understand the inhibition of AChE and development of effective inhibitors, which can also target other important pathways of AD hallmark.[8] In this paper, we have designed seven octapeptides (OPs) from the PAS and CAS binding site of AChE. We checked the active amino acids in both sites followed by identification of the most interacting amino acids by using relative frequency of amino acid contacts by Faure et al.[9] Thereafter, we performed molecular docking experiments in Autodock Vina 1.1.2[10] with designed peptides at AChE sites and found that peptide OP5 (NFDVLTEQ) binds more strongly among other designed peptides with maximum binding energy (BE) of −10.2 kcal mol^{-1}. Then we further shuffled this sequence and made a small library of 10 peptides to check the positional impact of different amino acids. We have also performed various in vitro and in vivo studies with the most promising candidate (i.e., OP5), which shows that this peptide binds to both the sites of

Received: May 26, 2018
Accepted: July 17, 2018
Published: July 17, 2018

DOI: 10.1021/acschemneuro.8b00253
ACS Chem. Neurosci. 2018, 9, 2838−2848

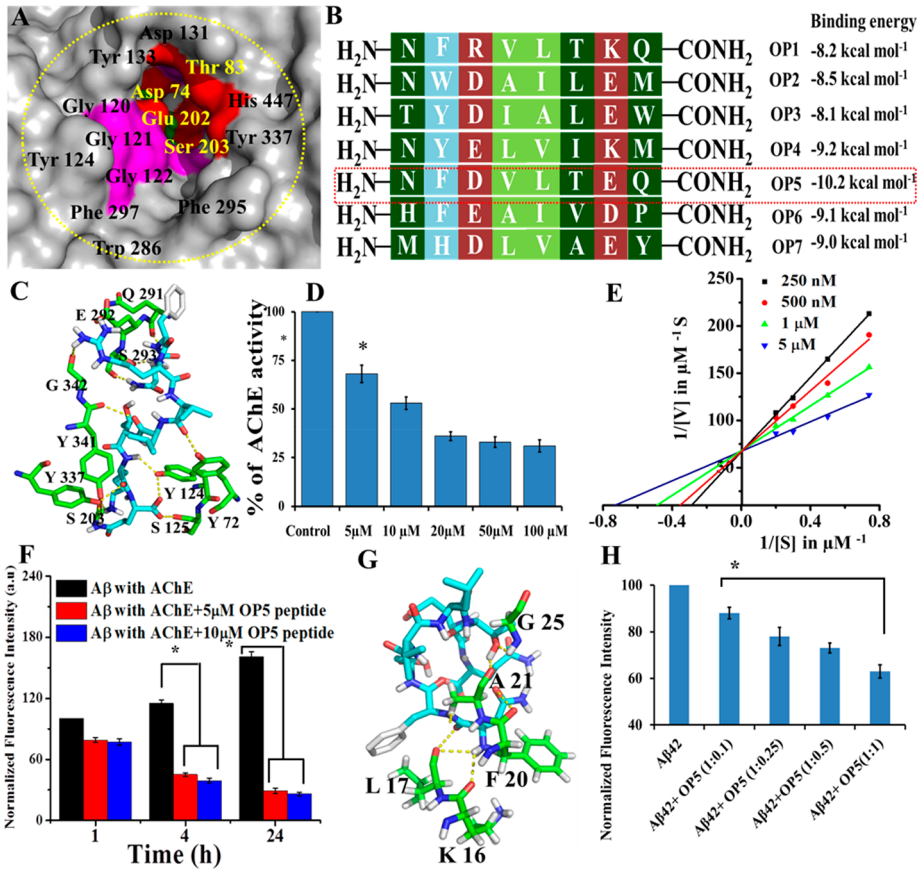

Figure 1. (A) Docking image showing various key amino acids of PAS and CAS binding site of AChE, which includes TYR 337, TYR 341, HIS 447, GLY 342, GLU 292, PHE 295, PHE 295, and SER 203 of the CAS binding site and VAL 132, TYR 124, TRP 286, SER 203, THR 83, TRP 86, ASP 74, GLY 122, and GLU 202 of the PAS binding site. (B) Seven different peptides have been designed from PAS and CAS binding site using the concept of relative frequency of amino acids contacts. (C) Molecular docking of NFDVLTEQ (OP5) at CAS and PAS binding site of AChE results in interaction of OP5 with some amino acids "(Q291, E292, S293, G342, Y341, Y337, S203, Y124, S125, and Y72) of that pocket. (D) Bar diagram shows inhibitory effect of OP5 peptide on AChE enzyme activity using various OP5 concentrations (IC_{50}, 7.3 μM, error bar corresponds to standard deviation of the values, *p < 0.05, performing two tailed Student's t test). (E) Lineweaver–Burk plot of AChE showing competitive inhibition with various concentrations (5, 1, 0.5, and 0.25 μM) of OP5 in different substrate concentrations (87.5–700 μM). (F) AChE induced Aβ aggregation inhibition by various OP5 peptide concentration. Error bars correspond to standard deviation of the value (*p < 0.001, performing one way ANOVA). (G) OP5 binds at the 17–21 region of Aβ and the interaction partners are K16, L17, F20, A21, and G25 (binding energy of −4.7 kcal mol^{-1}). (H) Inhibition of Aβ aggregation by using different concentrations of OP5 peptide monitored with thioflavin-T. Error bar corresponds to standard deviation of the value (*p < 0.05, performing two way Student's t test).

AChE (i.e., CAS and PAS) and inhibits amyloid aggregation by binding at the 17–21 region of the Aβ peptide. This peptide even interacts with tubulin and increases tubulin polymerization and the expression of acetylated tubulin. In PC12 derived neurons, this peptide is nontoxic in nature, shows excellent neuroprotection against anti-NGF mediated toxicity, and has the ability to cross the blood-brain barrier (BBB) effectively.

2. RESULTS AND DISCUSSION

2.1. Computational Approach for the Designing of Different Peptide Inhibitors. We have adopted a new strategy to develop AD therapeutics from the CAS and PAS site of AChE, as this is the key enzyme in the cholinergic nervous system and has a plausible cross-talk with the Aβ aggregation pathway. We have found some important amino acids known to interact with different inhibitors such as galantamine, huperzine, and donepezil, around the CAS and PAS binding site of the AChE enzyme (PDB ID 4EY6)[11] shown in Figure 1A. Afterthat, we designed one octapeptide (OP) "NFRVLTKQ" from the relative frequencies of the amino acids' interaction.[9] It is documented before that the 17–21 hydrophobic region of the Aβ peptide is mainly responsible for its aggregation and any peptide or small molecule that binds to this region can be a potent amyloid aggregation inhibitor.[12] Therefore, some nonpolar hydrophobic amino acids (e.g. valine, leucine, and phenylalanine) have been incorporated in the designed sequence deliberately, to make this peptide an amyloid aggregation inhibitor. Further, we modified this peptide sequence using the relative frequencies of the amino acid contacts and designed six more sequences following the same strategy to find out the most optimistic OP among these seven designed OPs (Figure 1B). From molecular docking study of these seven peptides with AChE enzyme at the CAS and PAS binding region, we have identified that NFDVLTEQ (OP5) is the most promising candidate having maximum binding energy (−10.2 kcal mol^{-1}) among the seven designed OPs (Figure S1A–G). Binding energies of all the OP analogues are listed in Figure S1H. The binding of OP5 is stabilized by the H-bonding interaction of amino acids S125, Y124, S203, and Y72 of the PAS binding site and Y337, G342,

DOI: 10.1021/acschemneuro.8b00253
ACS Chem. Neurosci. 2018, 9, 2838–2848

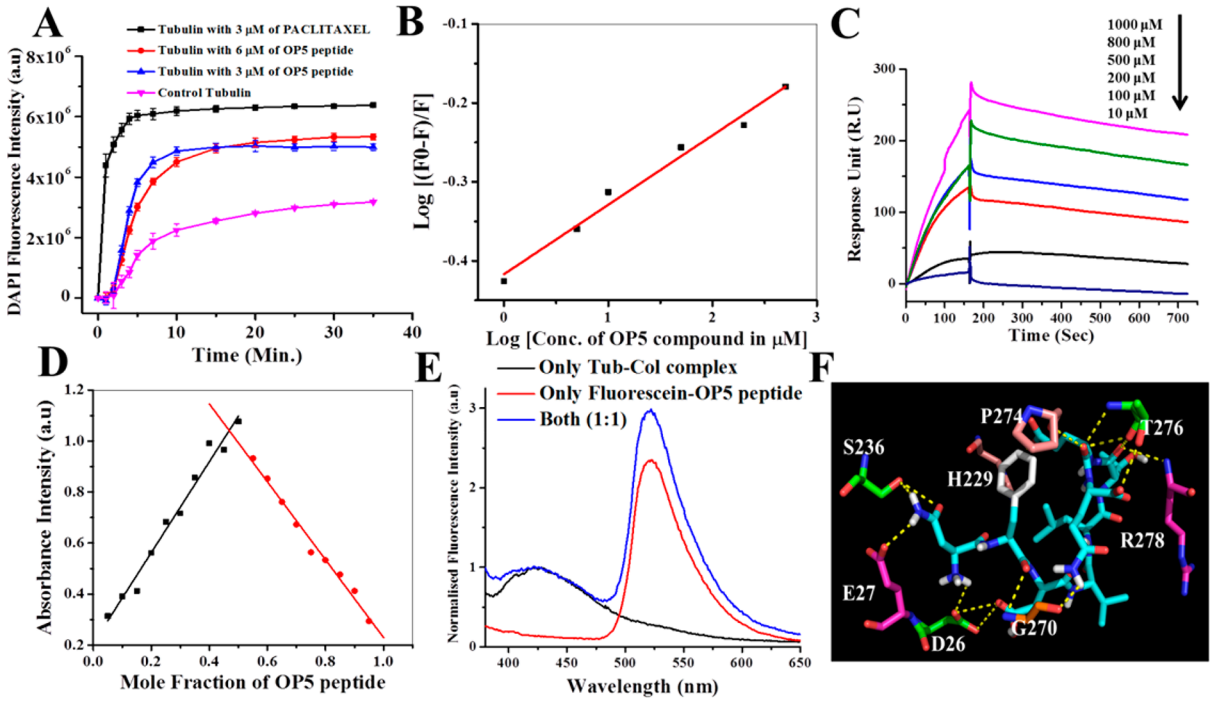

Figure 2. (A) Microtubule assembly assay using various concentration of OP5 peptide (3 and 6 μM) and paclitaxel (3 μM). (B) Determination of binding constant (K_b) by measuring the intrinsic tryptophan fluorescence quenching value of tubulin with increasing concentration of OP5. (C) Kinetic analysis of OP5 peptide binding with tubulin monitored by SPR sensogram on a NTA biosensor chip surfaces. (D) Stoichiometric binding of OP5 peptide with tubulin, showing (1:1) binding in Job plot. (E) FRET study between Tubulin-colchicine complex (donor) and Fluorescein-OP5 (acceptor) to find the binding region of OP5 in tubulin. (F) Various amino acids around the taxol site of tubulin interact with OP5 peptide.

E292, and S293 of the CAS binding site of the AChE enzyme (Figure 1C). The peptide sequence and chemical structure of OP5 peptide are shown in Figure S2. So, the above computational analysis suggests that OP5 peptide is binding and interacting at the CAS and PAS binding site simultaneously. Therefore, we further shuffled the optimized sequence and constructed a small library of 10 peptides to find out the positional impact of the various polar and non-polar (hydrophobic) amino acids. After performing molecular docking of all the peptides with AChE, we found that OP5 was the most promising peptide among them (Table S3).

2.2. Synthesis, Purification, Characterization, and Fluorescein Attachment of the Most Promising Octapeptide (OP5) and Its Scrambled Peptides. As the OP5 peptide is showing maximum binding energy with AChE enzyme, we carried our further studies with this peptide only. For control experiment, we have taken another two peptides from the constructed Table S3 (NLQVFEDT, scramble 1; and VDNFLETQ, scramble 2) having binding energy close to OP5. These three peptides were synthesized in a microwave-assisted peptide synthesizer (CEM Liberty 1) by following a solid-phase peptide synthesis (SPPS) method and using Rink amide AM resin. In addition, a brain penetrating peptide (YPFF) was synthesized following the same procedure mentioned above. We have also done the fluorescein attachment and N-acetylation of OP5 peptide by SPPS to perform the cellular uptake and serum stability of the peptide, respectively. All the crude peptides have been purified by reverse phase HPLC with C18 column and characterized by MALDI-TOF mass spectrometry (Figures S4–S8).

2.3. Acetylcholinesterase Inhibition by OP5 Peptide. First, we have checked the effect of OP5 in the inhibition of AChE and found that it has a significant inhibitory activity (IC50–7.34 μM) on AChE enzyme (Figure 1D).[13] Therefore, we further investigated the mechanistic aspects of inhibition of AChE activity by OP5. We calculated the substrate–velocity curve with varying concentrations of OP5 (0.25–5 μM) with different substrate (acetylthiocholine) concentrations (87.5 to 700 μM) to analyze the binding site of this peptide and understand the mechanism of AChE inhibition. From the Lineweaver–Burk plot (Figure 1E), we documented the changing values of K_m (negative reciprocal of X-intercept) while V_{max} (reciprocal of Y-intercept) remained the same with increasing concentrations of OP5,[13] indicating its binding with AChE at CAS site in a competitive manner. It is already documented before that Aβ peptide binds at the hydrophobic PAS binding pocket of the AChE and induces its aggregation. This event can be inhibited by a suitable inhibitor, which has ability to interact with either CAS or PAS binding site of AChE. Thus, we evaluated whether OP5 has any inhibitory effect on AChE induced Aβ aggregation or not. Co-incubation of OP5 and Aβ (1–42) with AChE for 24 h resulted in significant decrease of amyloid aggregation with increasing concentration of OP5 (5, 10 μM) (Figure 1F). This result clearly indicates that OP5 not only inhibits AChE activity but also has a substantial inhibitory effect on AChE induced Aβ aggregation.

2.4. Molecular Docking Study of OP5 Peptide with Amyloid-β Peptide. We further investigated the binding potential of OP5 with Aβ (PDB ID 1IYT)[12] through a molecular docking study.[10] We found that OP5 has very good binding affinity with Aβ peptide, having a binding energy of -4.7 kcal mol^{-1}. The amino acids of Aβ peptide that shows H-bonding interaction with OP5 peptide are shown in Figure 1G. So, this result clearly suggest that OP5 is binding at the 16–21

DOI: 10.1021/acschemneuro.8b00253
ACS Chem. Neurosci. 2018, 9, 2838–2848

hydrophobic stretch of Aβ peptide, which is mainly responsible for Aβ aggregation.[14]

2.5. Thioflavin T (ThT) Assay to Monitor the Inhibition of Amyloid Aggregation by OP5. Now, to justify this computational result, we performed an in vitro ThT assay with Aβ,[15] where we agitated Aβ peptide solution with various concentrations of OP5 for 48 h and monitored the inhibition of amyloid aggregation with time. The results of this assay shows ∼40% decrease in ThT fluorescence (Figure 1H) in a 1:1 molar ratio of OP5 with Aβ peptide, which means significant inhibition of amyloid aggregation by OP5. Further, we compared this result with the inhibiton activity of curcumin, a known inhibitor of amyloid aggregation. It has been well documented before that curcumin has an IC_{50} of 0.8−1 μM in amyloid aggregated conditions.[16] Therefore, we have measured the inhibitory activity of both curcumin and OP5 at 1 μM concentration. The results suggest that in the case of curcumin ∼43% amyloid inhibition occurs, whereas only 17% inhibition of amyloid aggregation occurs for our OP5 peptide at 1 μM concentration after 48 h of incubation at 37 °C (Figure S9).

2.6. MD Simulation and FT-IR Study to Observe the Inhibition of Amyloid Fibrillation by OP5. Though the above two studies have already suggested that our peptide inhibits amyloid aggregation by binding at the 16−21 region of Aβ, we were keen to understand the interaction between OP5 and Aβ in real time using molecular simulation (MD simulation). For this purpose, we have placed two short peptides sequence "KLVFFAE" with OP5 in a cubic simulation box having volume of 4.5 × 4.5 × 4.5. We performed simulation for 20 ns and found that upto 15 ns these two short peptides is not forming any stable β-sheet structure (also seen from the conformational secondary structure profile diagram in Figure S10). In the control experiment, they formed stable β-sheet structure only after 2 ns of simulation (data not shown). This inhibition of Aβ aggregation was further supported by FTIR analysis[14] (Figure S11).

2.7. Tubulin Polymerization Assay. In AD, intracellular tubulin/microtubule is severely affected and disrupted. Therefore, we explored, whether OP5 can provide microtubule stabilization. For that purpose, we first performed microtubule assembly assay using purified tubulin with various concentrations of OP5 in the presence of GTP. We found enhancement of tubulin polymerization with increasing concentrations of OP5 indicating it is binding with intracellular tubulin, which helps in tubulin polymerization and provides substantial stability. Further, we compared this result with the polymerization effect of paclitaxel on tubulin as it is a well-known tubulin polmerization enhancer. We found that in case of paclitaxel, tubulin polymerized within 2 min whereas tubulin polymerization in prescence of our peptide has a lag phase of 1−2 min and then it starts polymerizing (Figure 2A).[17,18]

2.8. Intrinsic Tryptophan Quenching Experiment and Surface Plasmon Resonance (SPR) Study to Measure the Binding Affinity of OP5 with Tubulin. Thereafter, we calculated the binding affinity of OP5 with tubulin by measuring the intrinsic tryptophan fluorescence quenching value at various concentrations of OP5 using the modified Stern−Volmer equation.[19,20] We found that the fluorescence intensity of intrinsic tryptophan of tubulin is reduced upon addition of OP5. The calculated binding constant of OP5 with tubulin is 3.8×10^5 M^{-1} (Figure 2B). We also performed this experiment with two scrambled peptides and calculated the binding constant which is quite less than that of OP5 (Scr1: 1.19×10^4 M^{-1}, Scr2: 2.1×10^4 M^{-1}) (Figures S12 and S13A). Further, we also performed surface plasmon resonance (SPR) study to check the binding affinity of this peptide with tubulin. We found that the binding affinities (k_a) of OP5 and scrambled 2 are 1.6×10^4 and 1.79×10^3 M^{-1} s^{-1} respectively, which is slightly deviated from but similar to our earlier findings in tryptophan quenching study (Figures 2C and S13B).

2.9. Stoichiometric Binding of OP5 with Tubulin Determined by UV-Absorbance. As this OP5 peptide has a moderate binding with tubulin, we further calculated the stoichiometric binding ratio of OP5 peptide with tubulin by measuring the absorbance value of the tubulin-OP5 complex at 280 nm wavelength.[21] We recorded the absorbance of this complex with various mole fractions of OP5 and plotted different absorbance values of this complex in a Job plot (Figure 2D). We found that, at the breakage point, OP5's mole fraction is ∼48% which indicates 1:1 binding of OP5 peptide with tubulin.

2.10. Binding Region Determination of Peptide by FRET Study.[21] Then we performed a Förster resonance energy transfer (FRET) experiment,[21,22] where we observed significant FRET between the tubulin−colchicine complex (donor) and fluorescein−OP5 (acceptor) peptide (Figure 2E). Förster distance (R_0) between this donor−acceptor pair is 29.5 ± 1 Å.[21] The calculated distance (R_{DA}) between the tubulin−colchicine complex and fluorescein−OP5 peptide is 32 ± 1 Å, which indicates that OP5 binds to tubulin in a site which is ∼32 Å apart from the colchicine binding site in tubulin. So, these results suggest that the OP5 peptide binds close to the taxol binding pocket of β-tubulin.

2.11. Molecular Docking Study of OP5 Peptide with Tubulin. Then, we performed molecular docking study around the taxol binding pocket of tubulin (PDB ID 1JFF)[23] with OP5 to understand its binding efficiency and interacting amino acid partners around the taxol pocket. We found that the binding energy is moderate (−7.1 kcal mol^{-1}), which indicates binding of OP5 around the taxol site of tubulin. The interacting partners of that pocket are shown in Figure 2F.

2.12. Cellular Uptake and Cell Viability Assay of OP5 Using Differentiated PC12 Cells. In vitro assay revealed that OP5 inhibits Aβ aggregation and promotes tubulin polymerization significantly. Therefore, we continued our exploration and validation through cellular studies of OP5 on neurons. First, we observed the cellular uptake of OP5 in PC12 (rat pheochromocytoma cells) derived neurons and found significant uptake (Figure 3A−C), which led us to perform a series of cellular studies of OP5 in differntiated PC12 neurons. At first we evaluated the toxicity of OP5 in differentiated PC12 cells, which shows that OP5 is not toxic to the cells up to 100 μM concentration (Figure 3D). This data confirms that OP5 does not create intracellular toxicity although it is binding at the taxol binding pocket. This result can be explained by the previous observation where, in spite of binding moderately (1.6×10^4 M^{-1}) with tubulin in the taxol binding pocket, its strength of binding is significantly weaker (225 times lower at 4 °C and 47500 times lower at 37 °C) as compared to taxol (3.6×10^6 M^{-1} at 4 °C; 7.6×10^8 M^{-1} at 37 °C).[24,25] This observation is indeed interesting and indicates that our peptide unlike other taxol stabilizing drugs will not exhibit toxicity.

2.13. OP5 Induced Neurite Outgrowth Study in PC12 Derived Neurons. Interestingly, we also found from microscopic DIC images that neurons are healthy and neurites

DOI: 10.1021/acschemneuro.8b00253
ACS Chem. Neurosci. 2018, 9, 2838−2848

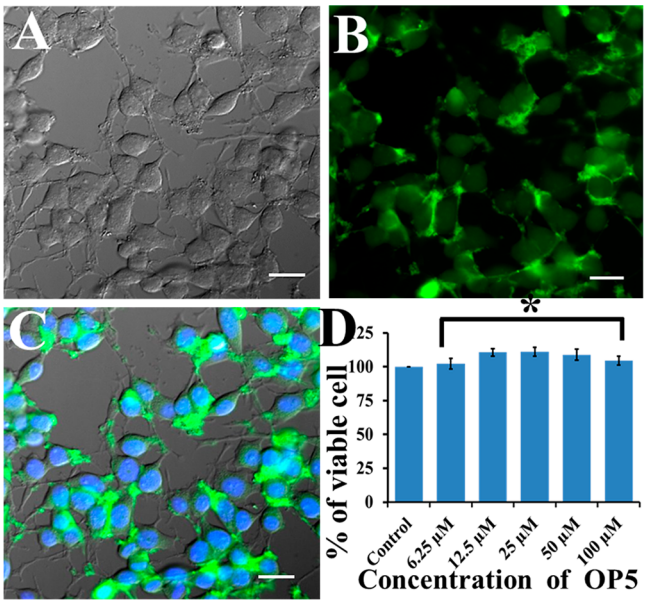

Figure 3. (A–C) Microscopic study in different channels (DIC and 488 nm) and their merged image shows significant cellular uptake of fluorescein–OP5 peptide in differentiated PC12 neurons. Scale bars correspond to 20 μm. (D) Cytotoxicity of OP5 peptide in differentiated PC12 derived neurons. This experiment was repeated thrice (n = 3), and error bar corresponds to standard deviation of the mean value (*p < 0.05, two tailed Student's t test).

are protruding upon treatment with 10 μM of OP5 without (Figure 4A,B) or with neuronal growth factor (NGF) (Figure

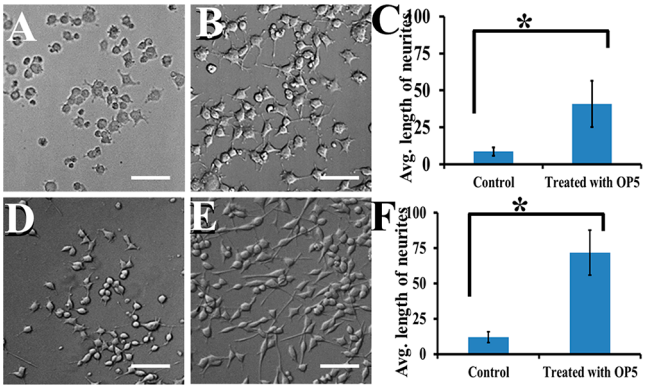

Figure 4. Neurite outgrowth of differentiated PC12 derived neurons (without neuronal growth factor, NGF) for (A) control cells and (B) cells treated with only OP5 peptide. (C) Average length of neurites for control cell and OP5 treated cells. Neurite outgrowth of differentiated PC12 derived neurons (using NGF) for (D) control cells and (E) cells treated with NGF+OP5 peptide. Scale bars correspond to 100 μm (F) Average length of neurites for control cell and OP5+NGF treated cells. Each experiment was repeated thrice (n = 3), and error bars correspond to standard deviation of the value (*p < 0.05, performing two tailed Student's t test).

4D,E). The average length of neurites in OP5 treated cells compared to untreated control is more, which indicates its role in promotion of neurite outgrowth (Figure. 4C,F). In AD, tau (a microtubule associated protein) gets hyperphosphorylated and forms neurofibrillary tangles which results in disruption of intracellular microtubule network.

2.14. In Vivo Microtubule Stabilization Assay Using Nocodazole Based Depolymerization. Therefore, we assessed the microtubule stabilization ability of OP5 on nocodazole depolymerized microtubules in PC12 derived neurons. PC12 derived neurons were treated with 10 μM nocodazole for 6 h. Medium was thereafter removed and replaced with a fresh medium containing 20 μM OP5 in one set and 10 μM paclitaxel (for comparison) in another set. For control cells, fresh medium without nocodazole was added. The intracellular microtubules were immunostained with tubulin specific antibody after another 2 h of incubation, followed by fluorescence microscopic imaging. Fluorescence microscopic images revealed that our OP5 stimulated microtubule assembly of the depolymerized microtubules, promoted neurite outgrowth, and is not toxic even at a high concentration of 20 μM (Figure 5I–L). On the other hand, paclitaxel induced further bundling of the depolymerized microtubules even at 10 μM concentration (Figure 5E–H) while no change in depolymerized microtubules were found in the untreated control cells (Figure 5A–D).

2.15. Immunoblotting Experiment. All this led to the finding that OP5 stimulates microtubule assembly and stabilizes leading to neuronal outgrowth. To further assess the in vitro effect of OP5 on microtubule stability, expression of acetylated tubulin (a known marker of microtubule stability) was quantified through immunoblotting. Significant increase in the expression level of acetylated tubulin in the OP5 treated cells compared to the scrambled peptides Scr1 or Scr2 but less than paclitaxel confirms that OP5 peptide is a good tubulin polymerizer that offers stability to the intracellular microtubules and binds just as much with it to not cause toxicity and bundling unlike paclitaxel (Figure 6A). Bar diagram of the previous immunoblotting quantification is shown in Figure 6B (*p < 0.05).

2.16. Neuroprotection Assay Using Anti-NGF. Next, neuroprotective potential of OP5 peptide was investigated by using nerve growth factor (NGF) deprived model where differentiated PC12 cells were treated with anti-NGF alone in one panel and coincubated along with different concentrations (1–50 μM) of OP5 in another panel.[26] This assay was performed by measuring the cell viability of the neurons against the anti-NGF mediated toxicity through MTT assay. We found that OP5 provides significant neuroprotection and helps to resurrect the neuronal morphology of the NGF deprived neurons (Figure 6C–E). This neuroprotection ability increases with increasing concentrations of OP5 peptide (Figure 6F). In comparison, paclitaxel or scrambled 2 peptide do not show any neuroprotection against anti-NGF mediated toxicity (Figures S14 and S15); in fact, paclitaxel has been earlier reported to cause neurotoxicity.[27]

2.17. Serum Stability of OP5 in Human Serum.[21,28] Since OP5 appeared as a good AChE inhibitor and confers significant neuroprotection, we were interested to explore its translational potential. As any therapeutic designed for targeting the brain, we first needed to confirm whether this is stable at physiological conditions and is able to cross the BBB. Therefore, we studied the serum stability of OP5 for evaluation of its suitability in an in vivo system by incubating OP5 in human serum solution at 37 °C and performing HPLC at every 2 h of incubation to monitor the percentage of intact peptide for up to 24 h. HPLC data reveals that OP5 was quite stable in human serum and 23% of the peptide was still remaining after 24 h of incubation (Figure 6G). The stability

DOI: 10.1021/acschemneuro.8b00253
ACS Chem. Neurosci. 2018, 9, 2838–2848

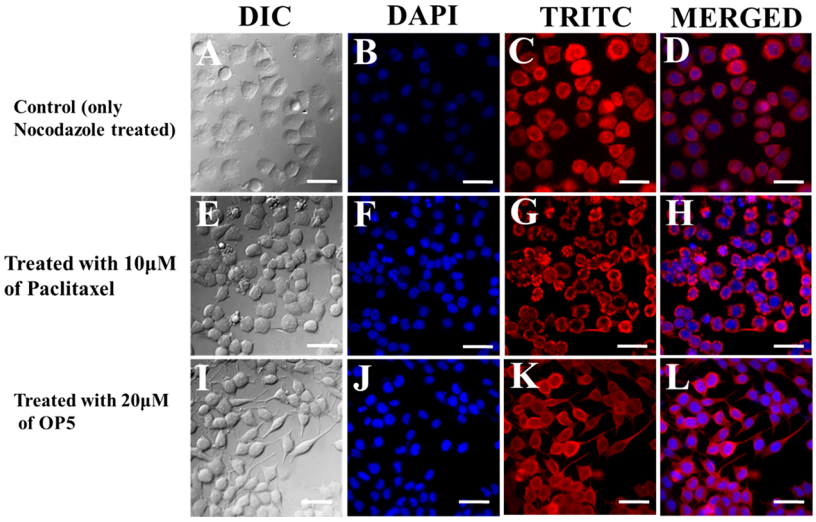

Figure 5. Nocodazole based depolymerization assay. Using nocodazole (a microtubule depolymerizer) to observe the neuroprotective activity of OP5 peptide and microtubule stabilizer paclitaxel. Top images indicate that cells have been treated initially with 10 μM nocodazole for 6 h and thereafter withdrawn. Microscopic images in different channels (DIC, DAPI, and TRITC) and their merged images reveal shrinkage of microtubule network for untreated control (A–D) and paclitaxel treated (E–H) PC12 derived neurons after nocodazole withdrawal. In the case of OP5, neurons are protruding and a significant amount of neuroprotection in differentiated PC12 neurons was observed (I–L). Scale bars correspond to 20 μm.

of the peptide is further increased up to ~50% when we used N-acetylated OP5 peptide instead of normal OP5 (Figure S16).

2.18. BBB Crossing Experiment with OP5.[29,30] Then we were curious to know whether OP5 can cross the BBB. For this purpose, OP5 (2.5 mM in saline solution, 100 μL) and vehicle (saline solution) were injected intraperitoneally 6 h prior to sacrifice. Brains were collected and extracts were prepared in acetonitrile solution (details are in Methods section 4.19). MALDI mass spectrum of OP5 treated brain extract revealed the presence of OP5 mass with Na^+ and K^+ ions (Figure. 7A), whereas in the case of vehicle treated (control) brain extract no such mass peak was observed (Figure S17). This result indicates that OP5 has the ability to cross the BBB. This method is well validated, as we have the molecular mass peak of YPFF (a brain penetrating peptide, taken from the Brain-peps database) after performing this experiment (Figure S18), whereas another scrambled peptide (NLQVFEDT; scramble 1) did not show any corresponding molecular peak in the mass spectrum (Figure S19) and could be cited as a negative control of the above procedure.

2.19. Effect of OP5 on Primary Cortical Neuron. Finally, we checked whether OP5 has any toxic effects in cultured primary cortical neurons. Primary cortical neuron culture has been performed following previously optimized protocol.[31,32] Microscopic images of treated and untreated cortical neurons indicate that there are no significant detrimental effects or any morphological changes (Figure 7B,C) confirming that OP5 does not have any toxic effect on primary neurons and the neuronal architecture were quite healthy similar to the control. The primary cortical neurons were further validated for their neuronal nature by staining them with anti-MAP2 antibody (MAP2 is a known marker for staining the dendrites of neurons). The OP5 treated neurons showed healthy MAP2 stained dendrites when viewed under the microscope (Figure. 7D).[32] This result further reinstated the neuronal character of the cortical neurons and the positive effect of OP5 on the neurons.

3. CONCLUSION

In summary, we have designed and developed a novel CAS binding octapeptide inhibitor for AChE enzyme, which inhibits Aβ aggregation and provides microtubule stabilization and neuroprotection. At the cellular level, this octapeptide is noncytotoxic in nature, promotes neurite outgrowth, stabilizes the intracellular microtubules of differentiated PC12 neurons, and provides significant neuroprotection against NGF deprived neurons. Further, this OP5 peptide has the ability to penetrate the BBB, shows good serum stability, and maintains healthy morphology of the primary rat cortical neurons. These above results confirm that OP5 could be a good candidate for further in vivo studies in AD mice model and further development of potential AD therapeutics.

4. METHODS

4.1. Chemicals. All the Fmoc protected amino acids, Fmoc-Rink Amide AM resin, and *O*-(1*H*-benzotriazol-1-yl) *N*,*N*,*N*′,*N*′-tetramethyluronium hexafluorophosphate (HBTU) were purchased from Novabiochem. Piperidine, dimethyl sulfoxide (DMSO), diisopropylethylamine (DIPEA), diethyl ether (Et_2O), and 1-hydroxybenzotriazole (HOBT) were purchased from Spectrochem. Phenol, ethanedithiol (EDT), dichloromethane (DCM), trifluoroacetic acid (TFA), thioflavin-T (ThT), hydrogen peroxide (30% solution), acetone, and *N*,*N*′-dimethylformamide (DMF) were purchased from Merck. Acetonitrile was purchased from J. T. Baker. Methanol was purchased from Finar. 3-(4,5-Dimethylthiazol-2-yl)-2,5-diphenyltetrazolium bromide (MTT), kanamycin sulfate, 5(6)-carboxy fluorescein (Fluorescein), *N*,*N*′-diisopropylcarbodiimide (DIC), and Dulbecco's modified Eagle's medium (DMEM) were purchased from Sigma-Aldrich. Human recombinant NGF was purchased from Sigma (St. Louis, MO). Amyloid beta (1–42) was purchased from AnaSpec. Acetylcholinesterase assay kit (colorimetric) (ab138871) was purchased from Abcam. Neurobasal media supplemented with B27, pen/strep, and glutaMAX were bought from Gibco, Life Technologies. All compounds were used without further purification.

4.2. Identification of Interacting Amino Acids and Design of Small Library of Neuroprotective Octapeptides through Computational Technique. We have found the most interacting amino acids at the CAS and PAS binding site of the

DOI: 10.1021/acschemneuro.8b00253
ACS Chem. Neurosci. 2018, 9, 2838–2848

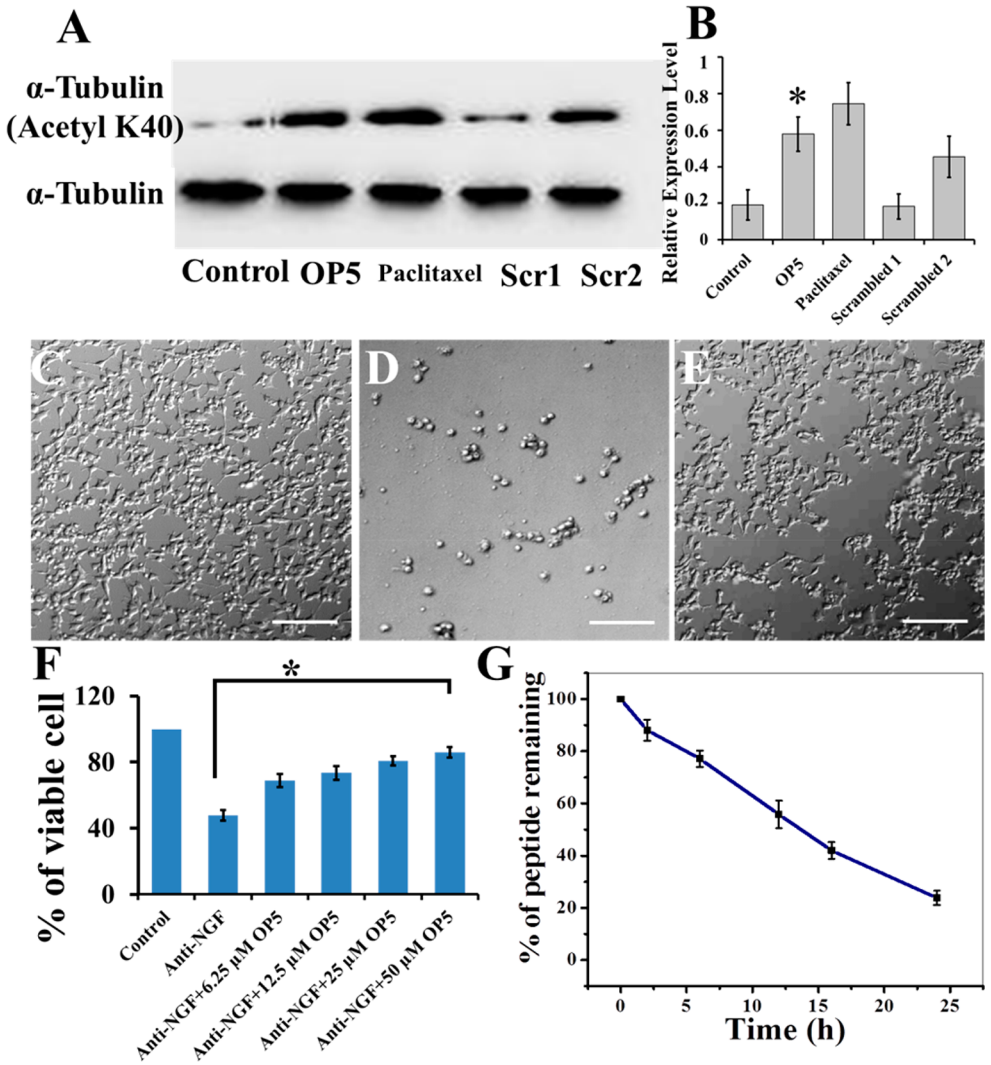

Figure 6. (A) Immunoblotting experiment with acetylated tubulin (control) in the presence of OP5, its scrambled peptides Scr1, Scr2, and paclitaxel. (B) Average densitometry plot of the immunoblot shown in bar diagram (*$p < 0.05$). Microscopic images of NGF treated control (C), anti-NGF treated (D), and Anti-NGF with OP5 peptide treated (E) differentiated PC12 neurons in DIC mode (scale bar corresponds to 100 μm). (F) Histogram showing anti-NGF study with various concentrations of OP5 peptide in differentiated PC12 neurons; error bar corresponds to standard deviation of the value (*$p < 0.05$, two tailed Student's t test). (G) Serum stability of OP5 peptide in human serum up to 24 h. Each experiment was repeated thrice ($n = 3$), and error bar corresponds to standard deviation of the mean value.

Acetylcholinesterase (AChE) by using its protein data bank structure (PDB ID 4EY6).[11] We have designed one octapeptide "NFRVLTKQ" from the relative frequencies of amino acid contacts of the most interacting amino acids of the CAS and PAS binding pocket of the AChE enzyme. Then, we further modified the peptide sequence and designed another six peptide sequences to find out the most promising candidate from this small library. Then we shuffled the most promising peptide to find out the positional impact of different amino acids of that sequence.

4.3. Molecular Docking Study for Calculation of Binding Energy of Octapeptides. Autodock-Vina version 1.1.2[10] was used to perform the docking study between the receptor AChE (PDB 4EY6),[11] amyloid beta (PDB 1IYT),[12] and tubulin (PDB 1JFF)[22] with octapeptides to find out the most potent peptide from the small octapeptide library, interaction with amyloid-β, and interaction with taxol pocket of β-tubulin, respectively. Affinity grids of volume 32 × 42 × 46, 40 × 26 × 54, and 20 × 20 × 16 were centered on the receptor acetylcholine esterase, amyloid beta, and tubulin for docking with seven different octapeptides. All the images were seen and produced in PyMOL (The PyMOL Molecular Graphics System, version 1.7.4 Schrödinger, LLC).

4.4. Synthesis, Purification, Characterization, and Fluorescein Attachment of the Most Promising Octapeptide (OP5). Synthesis of the most promising octapeptide (OP5), its fluorescein conjugation and N-acetylation, two scramble peptides NLQVFEDT (Scr1) and VDNFLETQ (Scr2) [having close docking energy], and a brain penetrating control peptide (YPFF) were performed in a Liberty 1 CEM microwave synthesizer following solid-phase peptide synthesis method by using Rink amide AM resin. At the time of synthesis, we have used 20% piperidine in DMF for Fmoc-deprotection. Finally, the crude peptide was cleaved of from the resin by using standard cleavage cocktail solution (TFA 91%, phenol 3%, EDT 3%, Milli-Q 3%) and purified using reverse phase HPLC and characterized by MALDI MS.

4.5. Acetylcholinesterase Inhibition of OP5 Peptide. Ellman's assay was performed with 4 different concentrations of OP5 to know the inhibitory effect of this peptide following previous reports.[13] Concisely, the enzyme was incubated with different concentrations of OP5 for 1 h at 37 °C. Then, we have recorded the absorption at 412 nm after mixing 0.01 M DTNB and 0.075 M ATC solution with enzyme exactly after 1.5 min of mixing. For control experiment, peptide was replaced by phosphate buffer. Also, to measure the kinetic value (substrate-velocity curve) of AChE inhibition by peptide we

DOI: 10.1021/acschemneuro.8b00253
ACS Chem. Neurosci. 2018, 9, 2838−2848

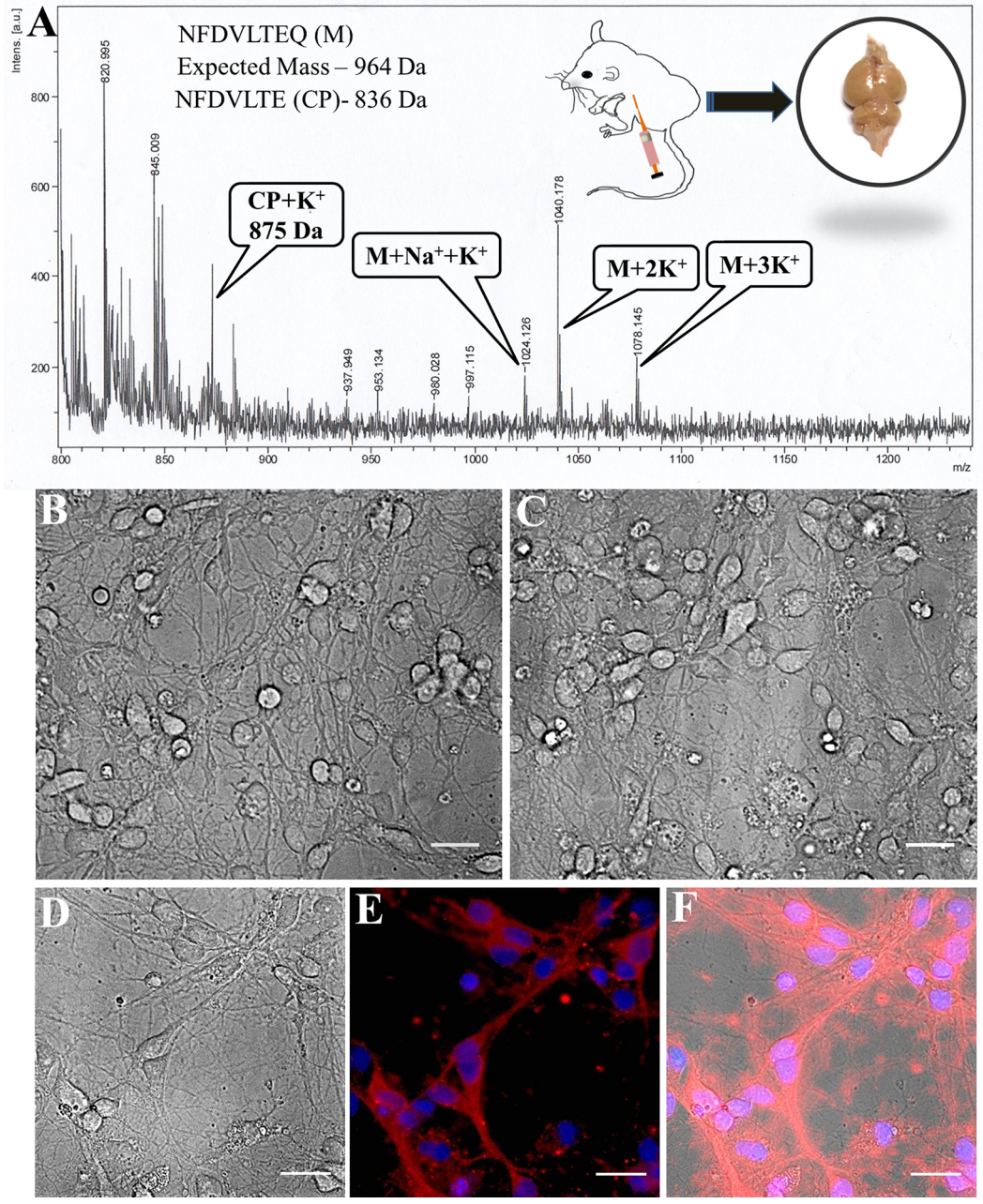

Figure 7. (A) MALDI-TOF mass spectra of mice brain extract after performing BBB crossing experiment with OP5 peptide. Expected mass (M) 964 Da, Observed mass 1024 Da $[M + Na + K]^+$, 1040 Da $[M + 2K]^+$, 1078 Da $[M + 3K]^+$, and cleaved peptide 875 Da $[CP + K]^+$. (B) Microscopic images of cortical neurons (control study) and (C) treated with OP5 peptide observed in DIC mode shows healthy neuronal network. Microscopic study of MAP2 staining of cortical neurons seen in (D) DIC mode, (E) merged 405 and 561 nm, and (F) merged DIC, 405, and 561 nm channel shows significant staining of a healthy neuronal network. Scale bars correspond to 30 μm.

have mixed different concentration of OP5 (0.25−2 μM) with different substrate (acetylthiocholine) concentrations (87.5−700 μM) to analyze the mechanism of inhibition. Then, we have plotted the Lineweaver−Burk plot to measure Vm and Km value of the inhibition.

4.6. Preparation of Amyloid-β(1−42) Peptide Stock Solution. Ten microliter aliquots of Aβ (1−42) peptide solution were prepared by mixing 1.0 mg of Aβ42 peptide in 400 μL of 1,1,1,3,3,3-hexafluoro-2-propanol and stored at −20 °C. At the time of experiment, 4 μL of this stock solution was dried under nitrogen gas, and then 1 μL of 1% NH_4OH was added into it and made the volume to 30 μL by using phosphate buffer saline (PBS buffer). The final concentration of the Aβ42 peptide solution was 80 μM. Then we further diluted this solution with PBS to adjust the concentration as per our experiment.

4.7. Acetylcholinesterase Induced and Plain Amyloid Aggregation Inhibition of OP5 Peptide. Inhibition of acetylcholinesterase induced Aβ and only Aβ peptide's aggregation by OP5 peptide (10 and 5 μM) were monitored by using 10 μM Aβ peptide in the presence of acetylcholinesterase enzyme (10 μM). For the control experiment, we did not mix peptide with this solution. We monitored the aggregation of Aβ peptide with ThT in a PTI QM-40 spectrofluorometer for 24 h. The excitation wavelength was 435 nm, and emission ranged between 460 and 650 nm.[13,15]

4.8. Protein Biochemistry. Tubulin was isolated, purified from goat brain (tubulin's concentration was maintained at 200 μM), and stored with glycerol according to a previously described procedure in our laborotory.[21]

DOI: 10.1021/acschemneuro.8b00253
ACS Chem. Neurosci. 2018, 9, 2838−2848

4.9. Tubulin Polymerization Assay. Tubulin polymerization assay was performed to measure the effect of OP5 on the polymerization rate of tubulin in the presence of GTP by measuring the DAPI (4′,6-diamidino-2-phenylindole) fluorescence. Fluorescence intensity of DAPI increases when it binds with microtubules. Therefore, by measuring the fluorescence intensity of DAPI, the polymerization rate of tubulin/amount of microtubule formation was quantified in the presence of OP5 peptide. A mixture of 10 μM DAPI in BRB80 buffer (BRB 80; 1 mM EGTA, 80 mM PIPES, 1 mM MgCl2, pH 6.9) containing 100 μM tubulin, 10 mM GTP, and various concentrations of OP5 peptide (3 and 6 μM) and paclitaxel (3 μM) were prepared. The excitation wavelength was 355 nm, and the fluorescence intensity of the solution was recorded from 400 to 600 nm wavelength for 60 at 5 min intervals in a PTI-QM40 spectrofluorimeter equipped with a Peltier system to control the temperature of the experiment.

4.10. Determination of Binding Affinity of OP5 by Measuring the Quenched Fluorescence Intensity of Intrinsic Tryptophan Residue of Tubulin. When a drug or small molecule binds to tubulin, the intrinsic tryptophan fluorescence intensity of tubulin is quenched. Therefore, we can measure the binding constant of this drug/small molecule by monitoring the fluorescence quenching value of tubulin. So, we measured the quenching value of tubulin's intrinsic tryptophan fluorescence in the presence of different concentrations of peptide. From this quenching value, the binding constant was determined using a modified Stern−Volmer equation. The emission spectra of 10 μM tubulin with different concentrations of peptide in BRB80 buffer in ice at 4 °C were recorded from 310 to 450 nm wavelength upon excitation at 295 nm using a PTI Quanta Master (QM-40) spectrofluorimeter equipped with a Peltier system.[21]

4.11. Binding Analysis of OP5 Peptide with Tubulin by Surface Plasmon Resonance (SPR) Study. Binding of OP5 and its scramble 2 with tubulin was analyzed by SPR experiment and using an NTA biosensor chip surface. Ni^{+2}, His(6)-streptavidin, and biotin-tubulin (20 μg/mL) were immobilized on the surface sequentially by flowing respective solutions. After that, a series of peptide solutions (10 μM to 1 mM) flowed over the tubulin immobilized NTA surface (flow rate was 30 μL/min). The kinetics of binding was analyzed by plotting the curve with a local fitting.

4.12. Stoichiometric Binding of OP5 with Tubulin Determined by UV-Absorbance. The stoichiometric ratio of OP5 binding with tubulin was determined by recording the absorbance of the tubulin−peptide complexes at 280 nm. We have taken the absorbance value of the complexes by mixing different mole fraction (0.05−0.95) of the peptide with various mole fraction (0.95−0.05) of tubulin in the solution. The molar ratio of binding was calculated using a Job plot.[21]

4.13. Binding Region Determination of Peptide by FRET Study.[21] FRET study was performed to find out the binding region of the peptide in tubulin. Recently, the tubulin−colchicine complex was used to find out the distance of fluorescein attached small molecule/peptide binds to tubulin as colchicine has a defined binding site in tubulin and has a significant overlap region with the fluorescein compound. The excitation wavelength was 355 nm, and the emission ranged from 450 to 650 nm. We recorded the emission of the tubulin−colchicine complex, fluorescein−OP5, and complex (mixed in 1:1 molar ratio). Efficiency of FRET was calculated by using the following equation:

$$\varepsilon_{FRET} = \frac{I_A}{\gamma I_D + I_A}$$

where I_A and I_D are the intensity of donor and acceptor molecules, respectively. Here, in this case we obtained from Figure 2d ε_{FRET} = 0.61.

Also, the reported Forster distance (R_0) between the tubulin−colchicine complex and fluorescein was ∼29.5 ± 1 Å.

$$R_{DA} = R_0\left(\frac{1-\varepsilon_{FRET}}{\varepsilon_{FRET}}\right)^{1/6}$$

Now, the distance (R_{DA}) between the donor tubulin−colchicine complex and acceptor fluorescein−OP5 was calculated using the above equation.

4.14. Cell Culture. The rat pheochromocytoma (PC12) cell line was a kind gift from Dr. Suvendra Nath Bhattacharyya. We cultured the PC12 cells in DMEM media containing 10% horse serum and 5% fetal bovine serum at 37 °C and 5% CO_2 atmosphere in our lab.

4.15. Cell Viability Assay Using Differentiated PC12 Cells. We used 96-well plates to culture the cells for 24 h. Then, serum free DMEM in 1% horse serum and 100 ng/mL NGF were used to differentiate the cells for 5 days. Following differentiation into neurons, different concentrations (100, 50, 25, 12.5, 6.25 μg/mL) of OP5 were incubated with cells for 24 h in a 37 °C and 5% CO_2 environment. Cell culture medium with 5 mg/mL MTT solution was mixed with the cells in each well for 4 h at 37 °C. Prior to reading the absorbance value, the media was removed and DMSO/MeOH (1:1) was used to solubilize the yellow formazan. A microplate ELISA reader (Thermo; MultiscanTM GO Microplate spectrophotometer) was used to read the absorbance value from the 96-well plate at a wavelength of 550 nm. The effect of peptide on differentiated PC12 cells was captured using a fluorescence microscope (IX83, Olympus) in DIC mode.[21]

4.16. Neuroprotection Assay Using Anti-NGF. The neuronal differentiation of PC12 cells was achieved by treating the cells with 100 ng/mL NGF in serum free DMEM containing 1% horse serum and incubating in a 37 °C and 5% CO_2 environment for 5 days. The cells were treated with anti-NGF (2 μg/mL) alone and with different concentrations of peptide after differentiation of cells into neurons for 20 h. Following incubation, MTT solution (5 mg/mL) was added to cells containing serum free media and incubated for 4 h at 37 °C. Then, we removed the incubation media and 1:1 MeOH/DMSO solution was added to each well. The plate was scanned using a microplate ELISA reader (Thermo; MultiscanTM GO Microplate spectrophotometer) at 550 nm.[26]

4.17. In Vivo Microtubule Stabilization Assay Using Nocodazole Based Depolymerization. To further understand the effect of OP5 on microtubule stability, its activity was tested in nocodazole depolymerized microtubules in PC12 derived neurons. The derived neurons were subjected to 10 μM nocodazole for 6 h. After that, the medium was removed and replaced with medium containing 20 μM OP5 in one set and 10 μM paclitaxel in another. For untreated control, fresh medium without any compound was added. After 2 h of incubation, microscopic imaging of the PC12 derived neurons was performed to assess its effect on microtubule stability. Briefly, 4% paraformaldehyde was used to fix the cells and incubated with 0.2% triton-X and 5% BSA in PBS for 1 h. After a wash with 1X PBS, cells were incubated with polyclonal anti-α-tubulin IgG antibody with dilution 1:300 for 2 h. Cells were then washed with PBS and secondary antibody (Cy3.5 preabsorbed goat anti-rabbit IgG) was added for 2 h having dilution 1:600. Then, cells were washed with 1× PBS and incubated with Hoechst 33258 (1 μg/mL) for 30 min before imaging. Microscopy was done using confocal microscope with a 40× objective (Olympus) and an Andor iXon3 897 EMCCD camera in 405 and 561 nm wavelengths laser lights.

4.18. Animal Models. C57BL/6J female mice were used for BBB permeability studies. For the primary cortical neuron culture studies, timed pregnant Sprague−Dawley rats were used. All the animal experiments have been performed following institutional animal ethics guidelines. All the animals used in this work were approved by institutional animal ethics committee [IICB/AEC/Meeting/Apr/2018/1].

4.19. Blood-Brain Barrier (BBB) Crossing Experiment with OP5.[29,30] Animals were divided in two groups (3 mice/group). Then 6 h prior to sacrifice, the mice were injected intraperitoneally with 100 μL of OP5 solution (in saline) at a dosage of 10 mg/kg body weight of mice. For the control study, mice were treated with 100 μL of saline solution (second group). After 6 h, animals were deeply

DOI: 10.1021/acschemneuro.8b00253
ACS Chem. Neurosci. 2018, 9, 2838−2848

anesthetized with ketamine (i.p.) and were sacrificed by transcardial perfusion, which was performed in order to drain the blood from the entire circulatory system. The mice brains were collected in PBS, and blood vessels and meninges were removed. Then dissection was performed in order to extract the brain cortical region for further analysis. Meninges free cortex was used to prepare brain homogenate, which homogenized in a mixture of acetonitrile and water (1:1). It was then centrifuged at 10000*g* for 10 min, and the supernatant was separated out from the pellet which has been previously reported to consist of brain vasculature, red blood cells, and brain nuclei.[33] After this capillary depletion, the brain vasculature free supernatant was taken for HPLC and mass analysis for the identification of OP5 mass and validation of its BBB permeability. Further, for the validation of our process, the experiment was repeated by taking a scramble peptide (Scr1) and a brain penetrating peptide (YPFF) from the Brain-peps database as a positive control.

4.20. Serum Stability of OP5 in Human Serum. Serum stability of OP5 peptide was performed to measure the stability of the peptide in physiological condition. It is extremely important to evaluate the bioavailability of a peptide before using them as drug candidates. We performed this experiment by using 50 μL of 200 μM OP5, 800 μL of human serum, and 150 μL of Milli-Q followed by incubation at 37 °C. After every 2 h, 100 μL of incubated solution was mixed with 100 μL of cold acetonitrile and kept at 4 °C for another 10−15 min. After that, mixture was centrifuged and filtrate was used for HPLC. We have repeated the experiment with N-acetylated OP5 to check whether the stability of the peptide was increased after acetylation. Finally, the change in intensity profile of OP5 and N-acetylated OP5's molecular peak in HPLC was plotted with time.[21,28]

4.21. Immunoblotting Experiment.[34] PC12 differentiated neurons were treated with 10 μM concentration of OP5 peptide and its two analogues, scrambled peptide 1 (Scr1: NLDFVTEQ) and scrambled peptide 2 (Scr2: NLDFVTEQ) and a well-known tubulin polymerizer paclitaxel for 12 h at 37 °C. After 12 h of treatment, cells were lysed on ice using RIPA cell lysis buffer supplemented with 1% protease inhibitor cocktail and then centrifuged at 12000*g* at 4 °C for 20 min. Bradford reagent was used to quantify the protein concentrations in the supernatants. The cell lysates were subjected to 12% SDS-polyacrylamide gel electrophoresis, then transferred onto PVDF membranes. The membranes were then probed with appropriate dilution of anti-alpha-tubulin (acetyl K40) primary antibody overnight at 4 °C. Membranes were then washed thrice with 1× TBS buffer and incubated with anti-mouse HRP-conjugated secondary antibody for 2 h at room temperature. All proteins were detected using Luminata Forte chemiluminescence reagent and quantified using densitometry adjusted against loading control alpha-tubulin.

4.22. Primary Cortical Neuron Culture. Primary cortical neurons were cultured as previously described.[31,32] Briefly, brains from E18 embryos of timed-pregnant Sprague Dawley rats were isolated, microdissected the brain cortices, digested, dissolved, filtered, and then suspended in MEM medium containing glucose (0.6 wt %/vol) and 10% horse serum. The suspended cells were then seeded on confocal dishes ((3−5) × 10^5/mL) coated with poly-D-lysine and cultured at 37 °C with 5% CO_2. After 4 h of incubation, medium was changed with neurobasal media supplemented with B27, GlutaMAX, and pen/strep. The cells were cultured for another 7 days and then treated with 10 μM OP5 peptide.

4.23. MAP2 Staining of the Primary Cortical Neurons. Primary cortical neurons were treated with 10 μM OP5 and immunostained with anti-MAP2 following a previously described protocol.[32] Briefly, the primary cortical neurons were fixed with 4% formaldehyde and then permeabilized using 0.3% Triton-X. Thereafter the fixed cells were incubated with primary mouse anti-MAP2 overnight at 2−8 °C. The cells were rinsed thrice with PBS the very next day and then incubated with secondary antibody Alexa Fluor 594 goat anti-mouse IgG for 2 h at 37 °C. After that, the cells were again rinsed with DPBS and the nucleus was stained using Hoechst 33258. The stained cells were then observed under confocal microscope with a 60× objective (Olympus).

4.24. Data Analysis. We used ImageJ and Origin 8.5 software to analyze the microscopic images and spectroscopic and statistical data, respectively. Statistical analysis was performed using two tailed Student's *t* test and one way ANOVA. Statistical values of different experiment varies between $*p \leq 0.05$ and $**p \leq 0.001$.

■ ASSOCIATED CONTENT

Supporting Information

This materials are available free of charge via the Internet at The Supporting Information is available free of charge on the ACS Publications website at DOI: 10.1021/acschemneuro.8b00253.

Molecular docking images and binding energies of various octapeptides, peptide sequence and molecular structure of OP5, Binding energies of various scrambles of OP5 peptide, HPLC chromatograms and MALDI-TOF mass spectrums of OP5 and its' scrambles, comparison of Aβ aggregation inhibition by OP5 with curcumin, MD simulation and FTIR study of amyloid fibril inhibition, Binding constant (K_b) determination of scrambled peptides, Anti-NGF study with various concentrations of OP5 and paclitaxel, microtubule depolymerisation assay with OP5, serum stability of N-acetylated OP5, and MALDI mass spectrums of different peptides BBB crossing experiment (PDF)

■ AUTHOR INFORMATION

Corresponding Author

*Tel: +91-33-2499-5872. Fax: +91-33-2473-5197/0284. E-mail: sghosh@iicb.res.in.

ORCID

Prasenjit Mondal: 0000-0003-0767-449X

Surajit Ghosh: 0000-0002-8203-8613

Author Contributions

P.M. performed molecular docking experiment for the screening of lead peptide from designed peptide library, synthesized and purified all the peptides, and performed various in vitro microtubule assays, e.g., microtubule assembly assay, tryptophan quenching experiment, SPR study, FRET experiment, and ThT assay. V.G. and G.D. performed the various cell based assays like cellular uptake, cell viability, neuroprotection, neurite-outgrowth, immunoblotting assay, and intracellular microtubule staining assay. G.D. and J.K. performed the primary cortical neurons experiment and MAP2 staining. K.P. helped P.M. for AChE enzyme inhibition assay. P.K.G. helped P.M. for the synthesis of scrambled peptides. Also, P.M. executed MD simulation experiment and various molecular docking studies with this peptide. P.M. and G.D. further helped S.G. in writing the manuscript. S.G. conceived the idea, supervised the project, and wrote the manuscript.

Notes

The authors declare no competing financial interest.

■ ACKNOWLEDGMENTS

We thank Dr. Konar, Dr. Biswas and IICB animal facility for the animal experiment. P.M. and P.K.G. thank CSIR, V.G. and J.K. thank DST-Inspire, GD thanks ICMR, and K.P. thanks UGC for awarding their fellowships. SG kindly acknowledges SERB, India (EMR/2015/002230) for financial assistance and CSIR-IICB for infrastructure.

DOI: 10.1021/acschemneuro.8b00253
ACS Chem. Neurosci. 2018, 9, 2838−2848

REFERENCES

(1) Ballard, C., Gauthier, S., Corbett, A., Brayne, C., Aarsland, D., and Jones, E. (2011) Alzheimer's disease. *Lancet 377*, 1019−1031.

(2) Šimić, G., Leko, M. B., Wray, S., Harrington, C., Delalle, I., Jovanov-Milošević, N., Danira, B. D., Buée, L., De Silva, R., Di Giovanni, G., Wischik, C., and Hof, P. R. (2016) Tau protein hyperphosphorylation and aggregation in Alzheimer's disease and other tauopathies, and possible neuroprotective strategies. *Biomolecules 6*, 6.

(3) Grossberg, G. T. (2003) Cholinesterase inhibitors for the treatment of alzheimer's disease: getting on and staying on. *Curr. Ther. Res. 64*, 216−235.

(4) Bartolini, M., Bertucci, C., Cavrini, V., and Andrisano, V. (2003) Beta-Amyloid aggregation induced by human acetylcholinesterase: inhibition studies. *Biochem. Pharmacol. 65*, 407−416.

(5) García-Ayllón, M. S., Small, D. H., Avila, J., and Sáez-Valero, J. (2011) Revisiting the role of acetylcholinesterase in alzheimer's disease: cross-talk with P-tau and β-Amyloid. *Front. Mol. Neurosci. 4*, 1−9.

(6) Carvajal, F. J., and Inestrosa, N. C. (2011) Interactions of AChE with Aβ aggregates in Alzheimer's Brain: Therapeutic Relevance of IDN 5706. *Front. Mol. Neurosci. 4*, 1−10.

(7) Silveyra, M. X., García-Ayllón, M. S., de Barreda, E. G., Small, D. H., Martínez, S., Avila, J., and Sáez-Valero, J. (2012) Altered expression of brain acetylcholinesterase in FTDP-17 human tau transgenic mice. *Neurobiol. Aging 33*, 23−34.

(8) Piazzi, L., Rampa, A., Bisi, A., Gobbi, S., Belluti, F., Cavalli, A., Bartolini, M., Andrisano, V., Valenti, P., and Recanatini, M. (2003) *J. Med. Chem. 46*, 2279.

(9) Faure, G., Bornot, A., and de Brevern, A. G. (2008) Protein contacts, inter-residue interactions and side-chain modelling. *Biochimie 90*, 626−639.

(10) Trott, O., and Olson, A. J. (2010) AutoDock Vina: Improving the speed and accuracy of docking with a new scoring function, efficient optimization, and multithreading. *J. Comput. Chem. 31*, 455−461.

(11) Cheung, J., Rudolph, M. J., Burshteyn, F., Cassidy, M. S., Gary, E. N., Love, J., Franklin, M. C., and Height, J. J. (2012) Structures of Human Acetylcholinesterase in complex with pharmacologically important ligands. *J. Med. Chem. 55*, 10282−10286.

(12) Crescenzi, O., Tomaselli, S., Guerrini, R., Salvadori, S., D'Ursi, A. M., Temussi, P. A., and Picone, D. (2002) Solution structure of the Alzheimer's disease amyloid beta-peptide (1−42). *Eur. J. Biochem. 269*, 5642−5648.

(13) Chen, X., Wehle, S., Kuzmanovic, N., Merget, B., Holzgrabe, U., König, B., Sotriffer, C. A., and Decker, M. (2014) Acetylcholinesterase Inhibitors with Photoswitchable Inhibition of β Amyloid Aggregation. *ACS Chem. Neurosci. 5*, 377−389.

(14) Biswas, A., Kurkute, P., Jana, B., Laskar, A., and Ghosh, S. (2014) An amyloid inhibitor octapeptide forms amyloid type fibrous aggregates and affects microtubule motility. *Chem. Commun. (Cambridge, U. K.) 50*, 2604−2607.

(15) Paul, A., Nadimpally, K. C., Mondal, T., Thalluri, K., and Mandal, B. (2015) Inhibition of Alzheimer's amyloid-β peptide aggregation and its disruption by a conformationally restricted α/β hybrid peptide. *Chem. Commun. 51*, 2245−2248.

(16) Yang, F., Lim, G. P., Begum, A. N., Ubeda, O. J., Simmons, M. R., Ambegaokar, S. S., Chen, P. P., Kayed, R., Glabe, C. G., Frautschy, S. A., and Cole, G. M. (2005) Curcumin Inhibits Formation of Amyloid Oligomers and Fibrils, Binds Plaques, and Reduces Amyloid in Vivo. *J. Biol. Chem. 280*, 5892−5901.

(17) Bonne, D., Heusele, C., Simon, C., and Pantaloni, D. (1985) 4',6-Diamidino-2-phenylindole, a Fluorescent Probe for Tubulin and Microtubules. *J. Biol. Chem. 260*, 2819−2825.

(18) Ghosh, J. G., Houck, S. A., and Clark, J. I. (2007) Interactive Domains in the Molecular Chaperone Human αB Crystallin Modulate Microtubule Assembly and Disassembly. *PLoS One 2*, e498.

(19) Gupta, K., and Panda, D. (2002) Perturbation of microtubule polymerization by quercetin through tubulin binding: a novel mechanism of its antiproliferative activity. *Biochemistry 41*, 13029−13038.

(20) Chakraborti, S., Das, L., Kapoor, N., Das, A., Dwivedi, V., Poddar, A., Chakraborti, G., Janik, M., Basu, G., Panda, D., Chakrabarti, P., Surolia, A., and Bhattacharyya, B. (2011) Curcumin recognizes a unique binding site of tubulin. *J. Med. Chem. 54*, 6183−6196.

(21) Jana, B., Mondal, P., Saha, A., Adak, A., Das, G., Mohapatra, S., Kurkute, P., and Ghosh, S. (2018) Designed tetrapeptide interacts with tubulin and microtubule. *Langmuir 34*, 1123−1132.

(22) Mondal, P., Chattoraj, S., Chowdhury, R., Bhunia, D., Ghosh, S., and Bhattacharyya, K. (2015) Direct observation of the growth and shrinkage of microtubules by single molecule Förster resonance energy transfer. *Phys. Chem. Chem. Phys. 17*, 6687−6690.

(23) Lowe, J., Li, H., Downing, K. H., and Nogales, E. (2001) Refined Structure of Alpha Beta-tubulin at 3.5 A Resolution. *J. Mol. Biol. 313*, 1045−1057.

(24) Díaz, J. F., Barasoain, I., and Andreu, J. M. (2003) Fast Kinetics of Taxol Binding to Microtubules. *J. Biol. Chem. 278*, 8407−8419.

(25) Matesanz, R., Barasoain, I., Yang, C., Wang, L., Li, X., de Inés, C., Coderch, C., Gago, F., Barbero, J., Andreu, J. M., Fang, W., and Díaz, J. F. (2008) Optimization of taxane binding to microtubules:binding affinity dissection and incremental construction of a high-affinity analog of paclitaxel. *Chem. Biol. 15*, 573−585.

(26) Adak, A., Das, G., Barman, S., Mohapatra, S., Bhunia, D., Jana, B., and Ghosh, S. (2017) Biodegradable Neuro-Compatible Peptide Hydrogel Promotes Neurite Outgrowth, Shows Significant Neuroprotection, and Delivers Anti-Alzheimer Drug. *ACS Appl. Mater. Interfaces 9*, 5067−5076.

(27) Bhutani, M., Colucci, P. M., Laird-Fick, H., and Conley, B. A. (2011) Management of paclitaxel-induced neurotoxicity. *Oncol. Rev. 4*, 107−115.

(28) Rajasekhar, K., Madhu, C., and Govindaraju, T. (2016) Natural Tripeptide-Based Inhibitor of Multifaceted Amyloid β Toxicity. *ACS Chem. Neurosci. 7*, 1300.

(29) Prades, R., Oller-Salvia, B., Schwarzmaier, S. M., Selva, J., Moros, M., Balbi, M., Grazú, V., de La Fuente, J. M., Egea, G., Plesnila, N., Teixidó, M., and Giralt, E. (2015) Applying the retro-enantio approach to obtain a peptide capable of overcoming the blood-brain barrier. *Angew. Chem., Int. Ed. 54*, 3967.

(30) Alonso, E., Vieira, A. C., Rodriguez, I., Alvariño, R., Gegunde, S., Fuwa, H., Suga, Y., Sasaki, M., Alfonso, A., Cifuentes, J. M., and Botana, L. M. (2017) Tetracyclic truncated analogue of the marine toxin gambierol modifies NMDA, tau, and amyloid β expression in mice brains: implications in AD pathology. *ACS Chem. Neurosci. 8*, 1358−1367.

(31) Xu, S. Y., Wu, Y. M., Ji, Z., Gao, X. Y., and Pan, S. Y. (2012) A modified technique for culturing primary fetal rat cortical neurons,. *J. Biomed. Biotechnol. 2012*, 1−7.

(32) Beaudoin, G. M. J., III, Lee, S. H., Singh, D., Yuan, Y., Ng, Y. G., Reichardt, L. F., and Arikkath, J. (2012) Culturing pyramidal neurons from the early postnatal mouse hippocampus and cortex. *Nat. Protoc. 7*, 1741−1754.

(33) Portran, D., Schaedel, L., Xu, Z., Théry, M., and Nachury, M. V. (2017) Tubulin acetylation protects long-lived microtubules against mechanical ageing. *Nat. Cell Biol. 19*, 391−398.

(34) Triguero, D., Buciak, J., and Pardridge, W. M. (1990) Capillary depletion method for quantification of blood-brain barrier transport of circulating peptides and plasma proteins. *J. Neurochem. 54*, 1882−1888.

DOI: 10.1021/acschemneuro.8b00253
ACS Chem. Neurosci. 2018, 9, 2838−2848